

Magnetic Excitations in the Spin Gap System TlCuCl_3

Akira OOSAWA*, Tetsuya KATO, Hidekazu TANAKA, Hidehiro UEKUSA¹,
Yuji OHASHI¹, Kenji NAKAJIMA², Masakazu NISHI² and Kazuhisa KAKURAI²

Department of Physics, Tokyo Institute of Technology, Oh-okayama, Meguro-ku, Tokyo 152-8551

¹*Department of Chemistry, Tokyo Institute of Technology, Oh-okayama, Meguro-ku, Tokyo
152-8551*

²*Neutron Scattering Laboratory, Institute for Solid State Physics, The University of Tokyo,
Tokai, Naka-gun, Ibaraki 319-1106*

(April 26, 2024)

Abstract

Single-crystal neutron inelastic scattering was performed in order to investigate the magnetic excitations in the spin gap system TlCuCl_3 . The constant- \mathbf{Q} energy scan profiles were collected in the $a^* - c^*$ plane. Three excitations are observed for $E \leq 15$ meV. One of the excitations is identified to be magnetic excitation. The lowest magnetic excitation with $E \sim 0.5$ meV occurs at $\mathbf{Q} = (1, 0, 1)$, as observed in KCuCl_3 . The dispersion relation of the magnetic excitation can be fitted to the dispersion formula derived from the weakly coupled dimer model. The intradimer interaction is evaluated as $J = 5.23$ meV, which coincides with the value estimated from the susceptibility data. However, one of the interdimer interactions obtained is so large that the weakly coupled dimer model is broken down.

PACS number 75.10.Jm, 78.70.Nx

Typeset using REVTeX

*E-mail: a-oosawa@lee.phys.titech.ac.jp

The quantum spin systems with spatial structures such as spin ladders, exchange-alternating chains and coupled antiferromagnetic dimer systems often have the excitation gap (spin gap) between the singlet ground state and the lowest excited triplet. Although the presence of the gap can be recognized through the exponential decrease of the susceptibility toward zero for $T \rightarrow 0$ and the zero magnetization plateau, the information on the magnetic excitation is necessary to elucidate the microscopic mechanism leading to the gap. The excitations from the singlet ground state essentially have quantum nature [1–4], and thus they cannot be described by the classical spin-wave theory. The magnetic excitations in the spin gap systems are new subject in magnetism.

This paper is concerned with the magnetic excitations in the spin gap system TlCuCl_3 [5,6]. This compound is isostructural with KCuCl_3 , which has a monoclinic structure (space group $P2_1/c$) [7]. The feature of the crystal structure is the double chain of edge-sharing CuCl_6 octahedra running along the a -axis, which are separated by Tl^+ ions. The magnitude of the spin gap Δ in TlCuCl_3 was evaluated from the magnetization process [6,8] and ESR measurements [9] as $\Delta = 0.65$ meV.

The magnetic excitations of isostructural KCuCl_3 have recently been measured by neutron inelastic scattering [10–13]. The dispersion relation obtained is well described in terms of the weakly coupled antiferromagnetic dimers [10–14]. Spins on the planar dimer Cu_2Cl_6 in the double chain form the antiferromagnetic dimer. The neighboring dimers couple along the double chain and in the cleavage plane $(1, 0, \bar{2})$. Since the crystal structures of TlCuCl_3 and KCuCl_3 are the same, it may be assumed that TlCuCl_3 is also the weakly coupled dimer system magnetically. However, there is a significant difference between their magnetic properties, *i.e.*, the spin gap for TlCuCl_3 is one-quarter of that for KCuCl_3 , while the saturation field for TlCuCl_3 is about two times as large as that for KCuCl_3 [6,15]. This suggests that the interdimer interactions in TlCuCl_3 is much stronger than those in KCuCl_3 . Thus we expect that the magnetic excitation in TlCuCl_3 is not necessarily similar to those in KCuCl_3 .

Quite recently the three-dimensional magnetic ordering in TlCuCl_3 has been observed in magnetic fields higher than the critical field $H_c = 5.7$ T [8]. Nikuni *et al.* [16] demonstrated

that the field-induced phase transition corresponds to the Bose-Einstein condensation of dilute magnons. The magnon mass can be determined by the curvature of the dispersion around the lowest excitation at zero field. Thus, it is worth while investigating the magnetic excitation in TlCuCl_3 by means of neutron inelastic scattering. Since large single crystals can be obtained, TlCuCl_3 is advantageous to neutron inelastic scattering.

TlCuCl_3 single crystals were grown from a melt by Bridgman method. The details of sample preparation were reported in reference 8. Since the precise structural analysis for TlCuCl_3 has not been reported, we performed the single crystal X-ray diffraction. The lattice parameters at room temperature were determined as $a = 3.9815\text{\AA}$, $b = 14.1440\text{\AA}$, $c = 8.8904\text{\AA}$ and $\beta = 96.32^\circ$. The atomic coordinates obtained are shown in Table I. As compared with the isostructural KCuCl_3 , the chemical unit cell of TlCuCl_3 is compressed along the a -axis and enlarged in the $b - c$ plane.

The neutron inelastic scattering was carried out using the ISSP-PONTA spectrometer installed at JRR-3M, Tokai. The constant- k_f mode was taken with fixed final neutron energy of $E_f=14.7$ meV. In order to gain intensity, collimations were set as open - monochromator - $80'$ - sample - $80'$ - analyzer - $80'$ - detector. The energy resolution is about 2 meV because of loose collimations. A pyrolytic graphite filter was placed after the sample to suppress the higher order contaminations. We used a sample with a volume of approximately 2.5 cm^3 . The TlCuCl_3 crystal has cleavage planes $(0, 1, 0)$ and $(1, 0, \bar{2})$. The sample was mounted in an ILL-type orange cryostat with its a^* - and c^* -axes in the scattering plane. Since TlCuCl_3 is a monoclinic crystal, the a^* - and c^* -axes are not orthogonal to each other. The crystallographical parameters $a^* = 1.6115$ $1/\text{\AA}$, $c^* = 0.71808$ $1/\text{\AA}$ and $\cos\beta^*=0.0967$ were used at helium temperatures. Excitation data were mainly collected at $T = 1.5$ K. All excitation spectra shown in this paper were taken by the constant- \mathbf{Q} energy scan in the energy range of 2~15 meV.

Figure 1 shows an example of the constant- \mathbf{Q} scan in TlCuCl_3 , which was measured at $\mathbf{Q}=(1.5,0,0)$ and at $T = 1.5$ K. The line widths expected from the spectrometer resolution are represented by horizontal bars. Three excitations are observed near $E = 3, 7$ and 12

meV. The scan profile was fitted with three Gaussians as shown by the solid line in Fig. 1. The background level was determined by the measurement for $E \leq -2$ meV, where no peak is appreciable. Sharp peaks much narrower than the resolution were excluded from the fitting.

Figure 2 shows the constant- \mathbf{Q} scan for $\mathbf{Q}=(1,0,0.8)$ measured at $T = 1.5$ K and 58 K. The intensity of the second excitation ($E \sim 6$ meV) is small for $\mathbf{Q}=(1,0,0.8)$. The intensity of the lowest excitation ($E \sim 4$ meV) decreases with increasing temperature, while the highest excitation ($E \sim 11$ meV) has the same intensity even at $T = 58$ K. From this result, the lowest excitation can be attributed to the magnetic origin.

In order to obtain the dispersion relation $\omega(\mathbf{Q})$, we collected scan profiles for selected reciprocal lattice points at $T = 1.5$ K. We confirmed that the periodicity of $\omega(\mathbf{Q})$ along the a^* -axis is the same as that of the nuclear reciprocal lattice, while the periodicity along the c^* -axis is doubled, as observed in KCuCl_3 [10,12]. Scan profiles were measured along $(h, 0, 0)$, $(h, 0, 1)$, $(1, 0, l)$, $(1.5, 0, l)$ and $(h, 0, 2h - 1)$ for $1 \leq l \leq 1.5$ and $0 \leq h \leq 1$. Figure 3 shows representative profiles. Three excitation peaks are observed in almost all of the profiles. The dispersion relation $\omega(\mathbf{Q})$ determined for TlCuCl_3 is shown in Fig. 4. We label these three excitations ω_1 , ω_2 and ω_3 , respectively. The lower ω_1 and ω_2 branches exhibit large dispersion, and intersect, while the highest one is not dispersive.

Here we discuss the present results. The spin-spin interactions in TlCuCl_3 can be expressed by the $S = 1/2$ Heisenberg model $\mathcal{H} = \sum_{\langle i,j \rangle} JS_i \cdot S_j$, because the susceptibilities and the magnetization curves for different field directions coincide, when normalized by the g -factors [5,6]. Therefore three excitations observed in TlCuCl_3 cannot be understood by the splitting of the triplet excitations due to the large anisotropy energy. In isostructural KCuCl_3 , we observed an dispersionless excitation with $E \sim 13$ meV, which is attributed to the phonon excitation [13]. Therefore the dispersionless ω_3 excitation $E \sim 12$ meV in TlCuCl_3 may also be attributed to the phonon excitation.

From the temperature dependence of the intensity of the ω_1 excitation, its origin was confirmed to be magnetic. Thus we see that the lowest magnetic excitation occurs at $\mathbf{Q} =$

(1, 0, 1) as observed in KCuCl_3 [10,12]. We measured the incoherent scattering at $\mathbf{Q} = (1, 0, 0.8)$, and confirmed that its tail is negligible for $E > 2$ meV. Using the data for $E > 2$ meV, we estimate the lowest excitation energy as $E_{\min} \sim 0.5$ meV by the Gaussian fit. The value of E_{\min} is compatible with the gap energy $\Delta = 0.65$ meV evaluated from the previous magnetization process [6,8] and ESR measurements [9]. Quite recently, the field-induced Néel ordering in TlCuCl_3 was observed by neutron elastic scattering [17]. In magnetic fields higher than the critical field of $H_c = 5.7$ T, magnetic Bragg peaks were observed at $\mathbf{Q} = (h, 0, l)$ with odd l in the $a^* - c^*$ plane. The result is consistent with the present observation.

The magnetic excitations in isostructural KCuCl_3 are well described by the weakly coupled dimer model [10–14]. Suzuki *et al.* argued that there exist two excitation modes in KCuCl_3 , because there are two kinds of dimers, which are located in the corner and the center of the chemical unit cell in the $b - c$ plane. The excitation modes are expressed as

$$\omega_{\pm}(\mathbf{Q}) = \sqrt{J^2 - JJ_{\pm}(\mathbf{Q})}, \quad (1)$$

with

$$J_{\pm}(\mathbf{Q}) = 2[J_a \cos(2\pi h) + J_{2a} \cos(4\pi h) + J_{2ac} \cos\{2\pi(2h + l)\}] \\ \pm 4[J_{abc} \cos\{\pi(2h + k + l)\} + J_{bc} \cos\{\pi(k + l)\}],$$

where J is the interaction in the dimer and J_a , J_{2a} , J_{2ac} , J_{abc} and J_{bc} are the effective interactions between a dimer and those located at $\mathbf{r} = \pm\mathbf{a}$, $\pm 2\mathbf{a}$, $\pm(2\mathbf{a} + \mathbf{c})$, $\pm(\mathbf{a} \pm \frac{1}{2}\mathbf{b} + \frac{1}{2}\mathbf{c})$ and $\pm(\pm\frac{1}{2}\mathbf{b} + \frac{1}{2}\mathbf{c})$, respectively. For the definition of the effective interdimer interactions, we follow reference 3. J_a and J_{2a} represent the interaction along the double chain, while J_{2ac} and J_{abc} are the interactions in the cleavage plane $(1, 0, \bar{2})$, in which the hole orbital $d(x^2 - y^2)$ lies. In KCuCl_3 , J_a , J_{2ac} and J_{abc} are dominant interdimer interactions [12–14]. The intensities are $I(\omega_+) \neq 0$ and $I(\omega_-) = 0$ for $\mathbf{Q} = (h, 0, l)$, while for $\mathbf{Q} = (0, k, 0)$, $I(\omega_+) = 0$ and $I(\omega_-) \neq 0$. In the present experimental condition, only the ω_+ mode is observable.

We fit eq. (1) for $\omega_+(\mathbf{Q})$ to the ω_1 branch in TlCuCl_3 , and obtain $J = 5.23$, $J_a = 0.21$, $J_{2a} = -0.06$, $J_{2ac} = 1.56$, $J_{abc} = -0.34$ and $J_{bc} = -0.09$ meV. Solid lines in Fig. 4 are

the fitting curves. The fitting looks well. The value of the intradimer interaction J agrees well with the value $J = 5.25$ meV estimated from the maximum susceptibility temperature $T_{\max} = 38$ K [5], *i.e.*, when the interdimer interactions are treated as the mean fields, the susceptibility is written as $\chi = 2Ng^2\mu_B^2\beta/(3 + \exp\beta J + \beta J')$, where N is the number of dimers, $\beta = 1/k_B T$ and J' is the sum of the neighboring interdimer interactions [18]. From this relation, we have $J/k_B T_{\max} = 1.60$.

The interaction parameters for TlCuCl_3 should be compared with those obtained for KCuCl_3 , $J = 4.34$, $J_a = 0.21$, $J_{2a} = -0.03$, $J_{2ac} = 0.45$, $J_{abc} = -0.28$ and $J_{bc} = -0.003$ meV [12–14]. The significant difference is seen in the value of J_{2ac} . J_{2ac} for TlCuCl_3 is four times as large as that for KCuCl_3 . In TlCuCl_3 the value of J_{2ac} is so large that the weakly coupled dimer model is broken down. Therefore, it is suggested that TlCuCl_3 is magnetically described as coupled exchange-alternating chains parallel to the $[2, 0, 1]$ direction rather than a weakly coupled dimer system.

The dispersion relation of the ω_- calculated with the interaction parameters obtained does not agree with the ω_2 branch. At present, the origin of the dispersive ω_2 excitation is unclear.

In conclusion, we have presented the results of neutron inelastic scattering on the spin gap system TlCuCl_3 . Three excitations were observed. The dispersion relation was determined in the $a^* - c^*$ plane. One dispersive magnetic excitation was identified. It was found that the spin gap corresponds to the excitation at $\mathbf{Q} = (1, 0, 1)$ as for KCuCl_3 . From the interaction parameters evaluated from the dispersion relation, it is suggested that TlCuCl_3 is magnetically a coupled exchange-alternating chain rather than a weakly coupled dimer system. The authors would like to thank N. Suzuki for useful discussion. This work was partially supported by a Grant-in-Aid for Scientific Research from the Ministry of Education, Science, Sports and Culture.

REFERENCES

- [1] E. Dagotto and T. M. Rice: *Science* **271** (1996) 618 and references therein.
- [2] M. Nishi, O. Fujita and J. Akimitsu: *Phys. Rev.* **B50** (1994) 6508.
- [3] B. Leuenberger, A. Stebler, H.-U. Güdel, A. Furrer, R. Feile and J. K. Kjems: *Phys. Rev.* **B30** (1984) 745.
- [4] Y. Sasago, K. Uchinokura, A. Zheludev and G. Shirane: *Phys. Rev.* **B55** (1997) 8357.
- [5] K. Takatsu, W. Shiramura and H. Tanaka: *J. Phys. Soc. Jpn.* **66** (1997) 1611.
- [6] W. Shiramura, K. Takatsu, H. Tanaka, M. Takahashi, K. Kamishima, H. Mitamura and T. Goto: *J. Phys. Soc. Jpn.* **66** (1997) 1900.
- [7] R. D. Willett, C. Dwiggin, R. F. Kruh and R. E. Rundle: *J. Chem. Phys.* **38** (1963) 2429.
- [8] A. Oosawa, M. Ishii and H. Tanaka: *J. Phys. : Condens. Matter* **11** (1999) 265.
- [9] H. Tanaka, T. Takatsu, W. Shiramura, T. Kambe, H. Nojiri, T. Yamada, S. Okubo, H. Ohta and M. Motokawa: *Physica. B***246-247** (1998) 545.
- [10] T. Kato, K. Takatsu, H. Tanaka, W. Shiramura, M. Mori, K. Nakajima and K. Kakurai: *J. Phys. Soc. Jpn.* **67** (1998) 752.
- [11] T. Kato, A. Oosawa, K. Takatsu, H. Tanaka, W. Shiramura, K. Nakajima and K. Kakurai: *J. Phys. Chem. Solids* **60** (1999) 1125.
- [12] N. Cavadini, W. Hengler, A. Furrer, H.-U. Güdel, K. Krämer and H. Mutka: *Eur. Phys. J. B* **7** (1999) 519.
- [13] T. Kato, A. Oosawa, K. Takatsu, H. Tanaka, W. Shiramura, K. Nakajima and K. Kakurai: in preparation.
- [14] N. Suzuki, Y. Fujimoto and S. Kokado: *Physica. B* in press.

- [15] K. Tatani, K. Kindo, A. Oosawa and H. Tanaka: Meeting Abstract of the Physical Society of Japan **53** (1998) Issue 2, Part 3, p. 543.
- [16] T. Nikuni, M. Oshikawa, A. Oosawa and H. Tanaka: submitted to Phys. Rev. Lett.; cond-mat/9908118.
- [17] H. Tanaka, A. Oosawa, T. Kato, K. Kakurai and A. Hoser: Meeting Abstract of the Physical Society of Japan **55** (2000) Issue 2, Part 3, p. 372.
- [18] K. Hara, M. Inoue, S. Emori and M. Kubo: J. Magn. Resonance **4** (1971) 337.

FIGURES

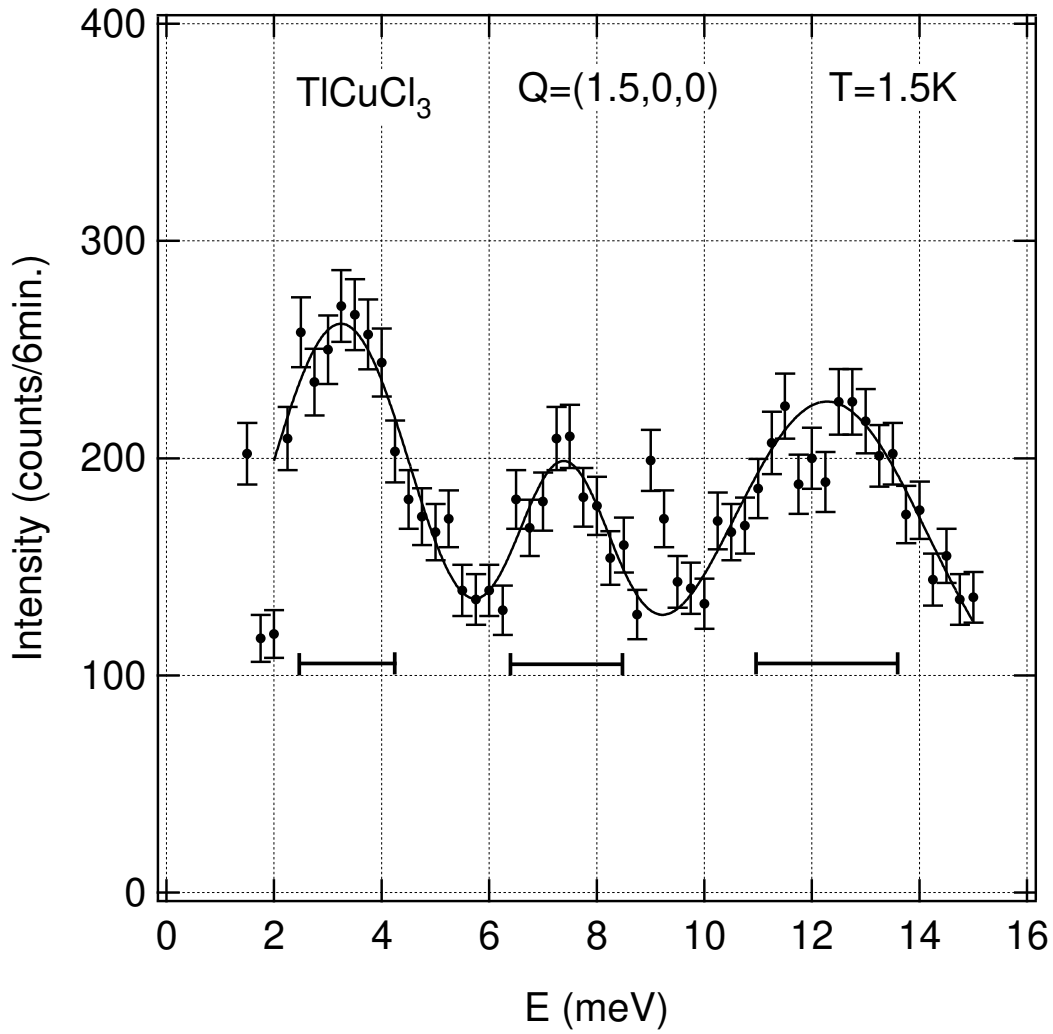


FIG. 1. The constant- \mathbf{Q} energy scan in TlCuCl₃ at $\mathbf{Q}=(1.5,0,0)$ and at $T = 1.5\text{K}$. The solid line is a fit using three Gaussians.

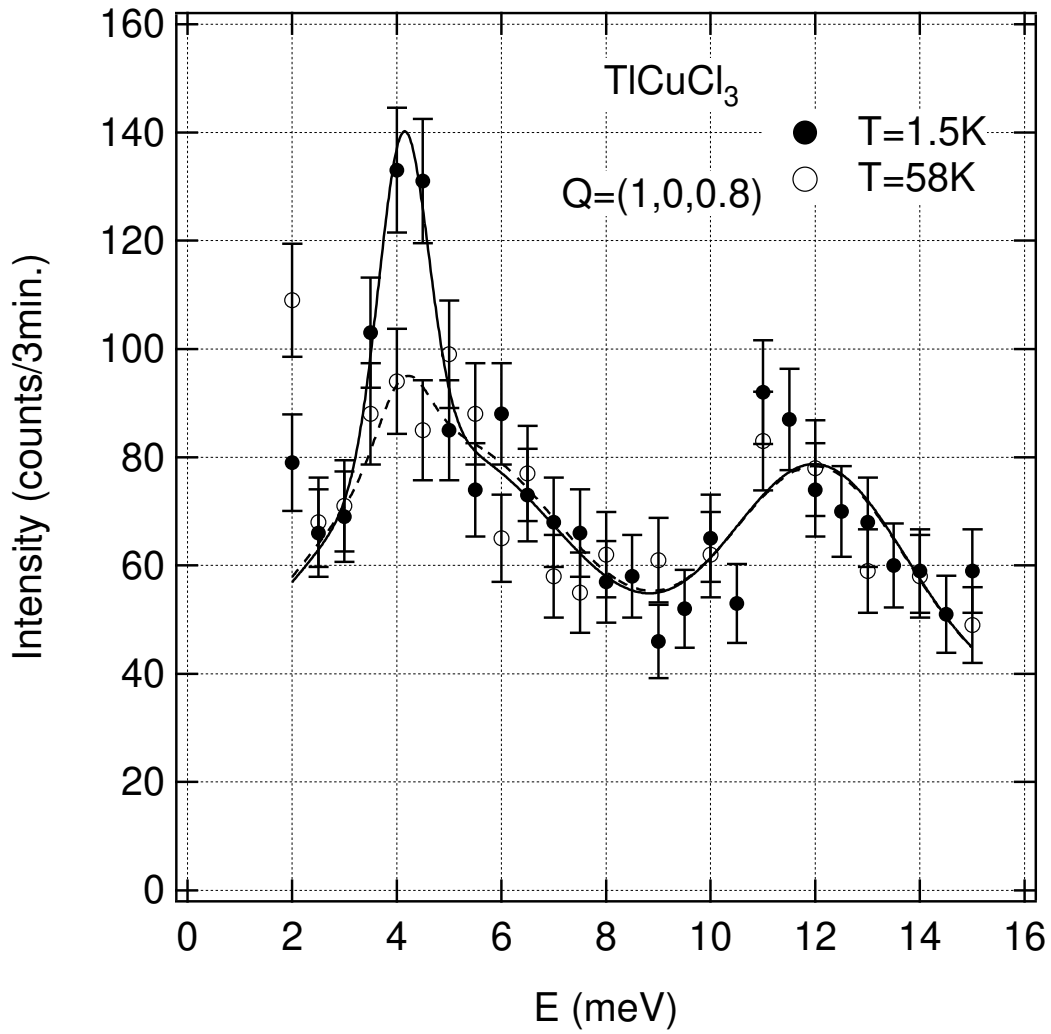


FIG. 2. The constant- Q energy scans in TiCuCl_3 at $Q=(1,0,0.8)$ at $T = 1.5\text{K}$ and 58K .

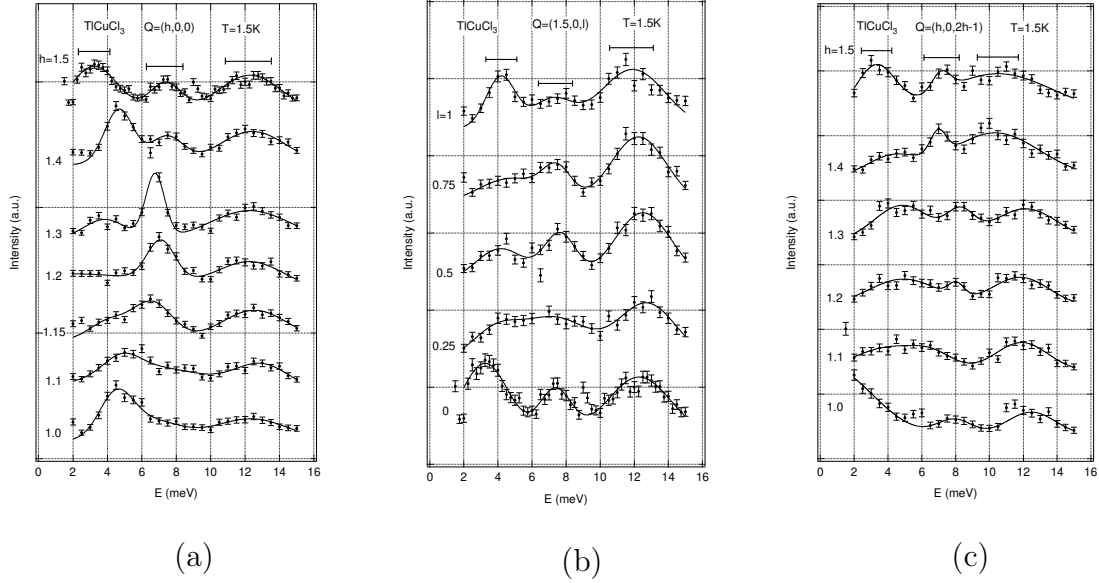


FIG. 3. Some profiles of the constant- \mathbf{Q} energy scans in TiCuCl_3 for \mathbf{Q} along (a) a^* -, (b) c^* - and (c) $(h, 0, 2h - 1)$ directions.

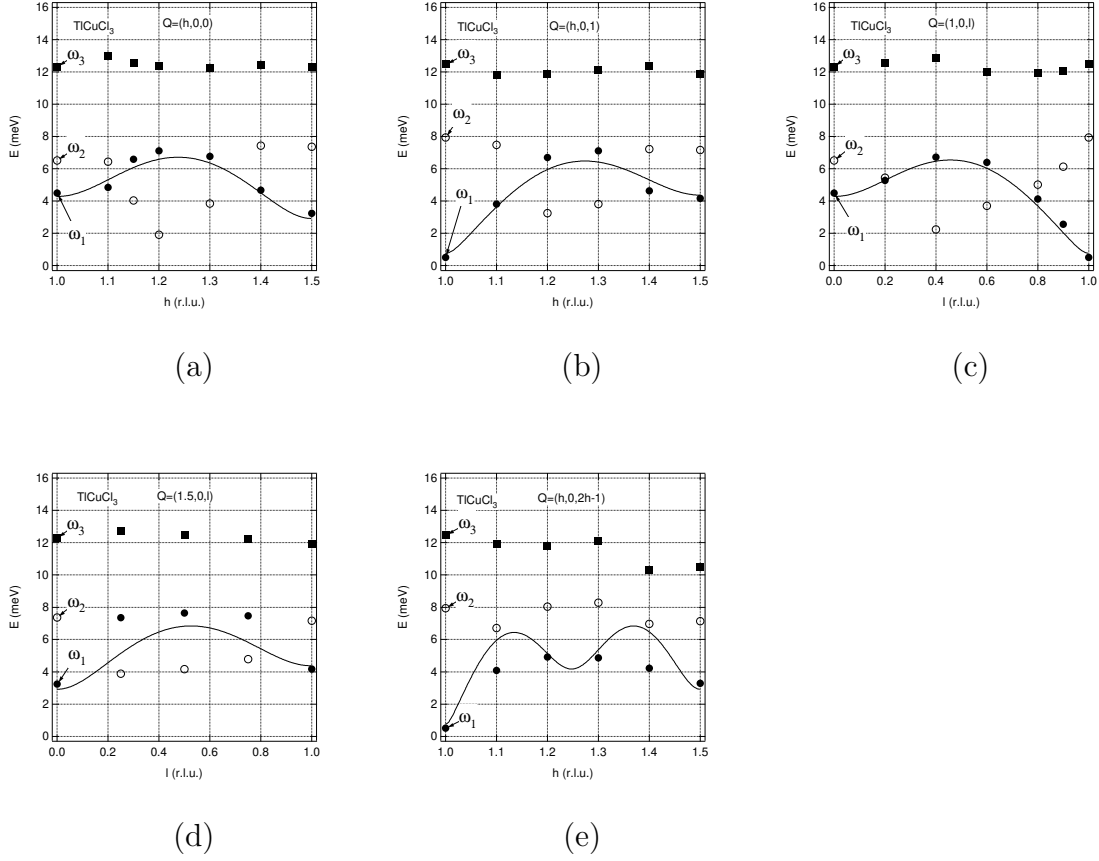


FIG. 4. The dispersion relations $\omega(\mathbf{Q})$ in TiCuCl_3 for (a) $\mathbf{Q} = (h, 0, 0)$, (b) $\mathbf{Q} = (h, 0, 1)$, (c) $\mathbf{Q} = (1, 0, l)$, (d) $\mathbf{Q} = (1.5, 0, l)$ and (e) $\mathbf{Q} = (h, 0, 2h - 1)$. Closed and open circles and rectangles denote the ω_1 , ω_2 and ω_3 modes, respectively. Solid lines are the fits for ω_1 mode using eq. (1) for $\omega_+(\mathbf{Q})$. See text for the fitting parameters.

TABLES

TABLE I. Atomic coordinates for TlCuCl_3 .

	x	y	z
Tl	0.7780	0.1700	0.5529
Cu	0.2338	0.0486	0.1554
Cl(1)	0.2656	0.1941	0.2597
Cl(2)	0.6745	-0.0063	0.3177
Cl(3)	-0.1817	0.0966	-0.0353